



# Mechanical properties, defects and electronic behavior of carbon nanotubes

M. Buongiorno Nardelli\*, J.-L. Fattebert, D. Orlikowski, C. Roland, Q. Zhao, J. Bernholc

*NC State University, Raleigh, NC 27695-8202, USA*

---

## Abstract

Using state-of-the-art classical and quantum simulations, we have studied the mechanical and electronic response of carbon nanotubes to external deformations, such as strain and bending. In strained nanotubes the spontaneous formation of double pentagon–heptagon defect pairs is observed. Tubes containing these defects are energetically preferred to uniformly stretched tubes at strains greater than 5%. These defects act as nucleation centers for the formation of dislocations in the originally ideal graphitic network and constitute the onset of further deformations of the carbon nanotube. In particular, plastic or brittle behaviors can occur depending upon the external conditions and tube symmetry. We have also investigated the effects that the presence of addimers has on strained carbon nanotubes. The main result is the formation of a new class of defects that wrap themselves about the circumference of the nanotube. These defects are shown to modify the geometrical structure and to induce the formation of nanotube-based quantum dots. Finally, we computed transport properties for various ideal and mechanically deformed carbon nanotubes. High defect densities are shown to greatly affect transport in individual nanotubes, while small diameter bent armchair nanotubes maintain their basic electrical properties even in presence of large deformations with no defects involved. © 2000 Elsevier Science Ltd. All rights reserved.

*Keywords:* A. Carbon nanotubes; D. Mechanical properties; Electronic properties

---

## 1. Introduction

The field of carbon nanotubes has seen an explosive growth in the recent years due to the substantial promise of these molecular structures for the use as high strength, light weight materials, superstrong fibers, novel nanometer scale electronic and mechanical devices, catalysts, and energy storage. Despite the potential impact that new composites based on carbon nanotubes would have in many areas of science and industry, a complete characterization of their mechanical and electrical properties is still insufficient.

One of the most important applications of carbon nanotubes is likely to take advantage of their outstanding mechanical properties, namely their extreme flexibility and strength at one-sixth the weight of steel. They have already demonstrated exceptional mechanical properties: the excel-

lent resistance of carbon nanotubes to bending has already been observed experimentally and studied theoretically [1,2]. Their high stiffness combines with resilience and the ability to reversibly buckle and collapse: even largely distorted configurations (axial compression, twisting) can be due to elastic deformations with no atomic defects involved [1–5]. We have focused on the theoretical analysis of the mechanism of strain release in carbon nanotubes under uniaxial tension, in an effort to address the question of the ultimate strength of these nanostructures. This issue requires the modeling of inherently mesoscopic phenomena, such as plasticity and fracture, on a microscopic, atomistic level, and constitutes a great challenge from the theoretical as well as experimental points of view.

## 2. Mechanical properties

We have been able to identify the first stages of the mechanical yield of carbon nanotubes via energetic relaxations and dynamical calculations using first principles

---

\*Corresponding author.

*E-mail address:* nardelli@nemo.physics.ncsu.edu (M. Buongiorno Nardelli).

methods and classical many-body potentials. The quantum simulations were carried out in the framework of a multigrid-based density-functional total energy method that uses a real-space grid as the basis [6,7]. The Perdew–Zunger parameterization of the Ceperley and Alder form [8] of the exchange and correlation energy was used. Non-local, norm-conserving pseudopotentials [9–11] were included using the Kleinman and Bylander approach [12]. In the classical simulations, carbon atoms were modeled with a classical many-body Tersoff–Brenner [13–15] potential that has been shown to reliably describe the main features of the mechanical response of carbon nanotubes [16,17].

Quantum molecular dynamics simulations have been performed in the canonical ensemble on a (5,5) tube under 10% tensile strain. The ideal nanotube has been initially relaxed in the strained geometry and subsequently heated to 1800 K. Multiple Nose–Hoover thermostats have been used to control the temperature during the simulation [18–20]. All the simulations were carried out on the massively parallel Cray T3D supercomputer with a time step of 0.64 fs for an overall time of ~6 ps. After an initial equilibration at 1800 K (~1 ps), a first precursor of a mechanical instability appears. A single C–C bond rotation generates a double pentagon–heptagon defect (5–7–7–5), as shown in Fig. 1.

The detailed knowledge of the formation and activation energies of these defects are of great importance to the understanding of the thermodynamics of such defects in both the mechanical response and the growth process of carbon nanotubes. The values of the formation energies of a (5–7–7–5) defect in an armchair (5,5) tube are summarized in Fig. 2, as obtained in our *ab initio* calculations.

From the above energetic considerations it follows that beyond a critical value of the tension of about 5%, an armchair nanotube under axial tension releases its excess strain via spontaneous formation of topological defects [16,17]. A transverse tension finds a natural release in the rotation of the C–C bond perpendicular to it (the so-called Stone–Wales transformation [21]) which produces two pentagons and two heptagons coupled in pairs (5–7–7–5) [16,17]. The appearance of a (5–7–7–5) defect can be interpreted as the nucleation of a degenerate dislocation loop in the planar hexagonal network of the graphite sheet. The configuration of this primary dipole is a (5–7) core attached to an inverted (7–5) core. The (5–7) defect behaves thus as a single edge dislocation in the graphitic plane. Once nucleated, the (5–7–7–5) dislocation loop can ease further relaxation by separating the two dislocation cores, which glide through successive Stone–Wales bond rotations [16,17]. This corresponds to a plastic flow of dislocations and gives rise to ductile behavior, as shown in Fig. 3. In contrast, in the case of a zig-zag nanotube, the same C–C bond will be parallel to the applied tension, which is already the minimum energy configuration for the strained bond. The formation of the Stone–Wales defect is

then limited to rotation of the bonds oriented 120° with respect to the tube axis. Our analysis shows that the formation energy of these defects is strongly dependent on curvature, i.e., on the diameter of the tube, and gives rise to a wide variety of behaviors in the brittle-vs.-ductile map of stress response of carbon nanotubes. In particular, the results of static energetics calculations and molecular dynamics simulations for (n,0) tubes of various diameters  $D$  at 10% strain are summarized in Fig. 4. Remarkably, the formation energy of the off-axis (5–7–7–5) defect (obtained via the rotation of the C–C bond oriented 120° wrt. tube axis) shows a crossover with respect to the diameter, and it is negative for (n,0) tubes with  $n < 14$  ( $D < 1.1$  nm). Similarly, the formation energy of this defect in chiral tubes of the (10, $m$ ) family (chosen as a particular example) is always negative, although it changes with the chiral angle  $\chi$ . This result implies that this geometrical transformation is still efficient in releasing the strain energy of the tube. The effect is clearly due to the variation in curvature, which in the small-diameter tubes makes the process energetically advantageous. Therefore, above a critical value of the curvature a plastic behavior is always possible and the tubes can be ductile.

From our calculations we can identify the full variety of elastic responses in strained carbon nanotubes. In particular, under high strain and low temperature conditions, all tubes are brittle. If, on the contrary, external conditions favor plastic flow, such as low strain and high temperature, (n, $m$ ) tubes with  $n, m < 14$  can be completely ductile, while larger tubes are moderately or completely brittle depending on their symmetry. These results are summarized in Fig. 5, where a map of the ductile vs. brittle behavior of a general (n, $m$ ) carbon nanotube under an axial tensile load is presented. There are four regions indicated by different shadings. The small hatched area near the origin is the region of complete ductile behavior, where the formation of (5–7–7–5) defects is always favored under sufficiently large strain. In particular, plastic flow will transform the tube section between the dislocation cores along paths parallel to the axes of Fig. 5. During the transformations, the symmetry will change between the armchair and the zig-zag type. The same transformations will occur in the larger (white) moderately ductile region. Tubes with indexes in this area are ductile, but the plastic behavior is limited by the brittle regions near the axes. Tubes that belong to the last two regions will always follow a brittle fracture path with formation of disordered cracks and large open rings under high tensile strain conditions.

In order to explore new possibilities in the design of nanotube-based devices using mechanically-assisted geometrical transformations, we have considered the effect of adatoms and addimers adsorption on strained nanotubes. The combination of such structures with strain turns out to be a natural route for the formation of different all-carbon nanotube-based quantum dots.

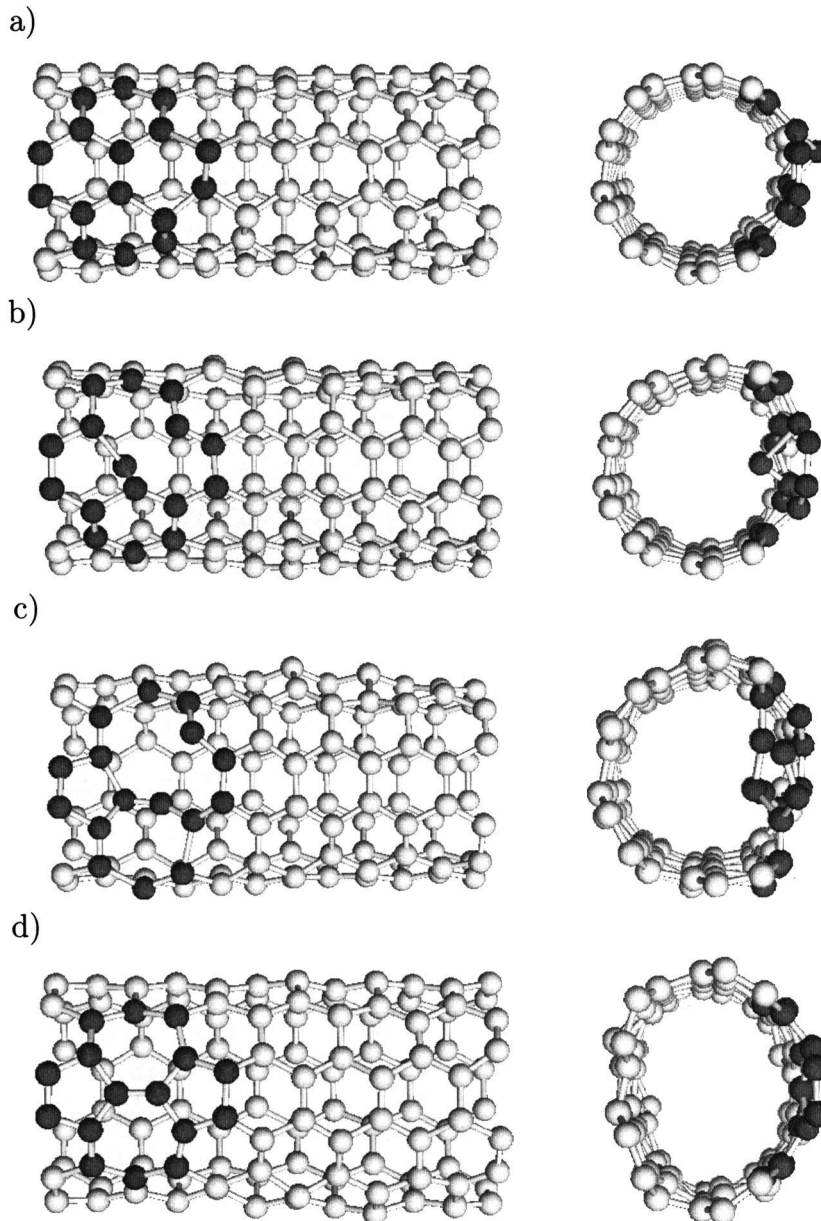


Fig. 1. Kinetic mechanism of (5–7–7–5) defect formation from an ab initio quantum mechanical molecular dynamics simulation for the (5,5) tube at 1800 K. The atoms that take part in the Stone–Wales transformation are highlighted in black. The four snapshots show the various stages of the defect formation: (a) system in the ideal configurations ( $t=0.00$  ps); (b) breaking of the first bond ( $t=0.10$  ps); (c) breaking of the second bond ( $t=0.15$ ); (d) the defect is formed ( $t=0.20$  ps).

Addimers are likely to be present in small amounts on as-grown carbon nanotubes, or they may be deposited there with an STM tip or other methods. Irrespective of the mechanism of adsorption, the addimers induce the formation of a new set of defects, consisting of rotated hexagons separated by (5–7) pairs from the rest of the tube, as shown in Fig. 6. This defect undergoes substantial further evolution under the appropriate strain conditions. Via the

successive rotations of C–C bonds, more hexagons are added to the initial defect, and if this process of adding hexagons were to continue, the defect structure would eventually wrap itself completely about the circumference of the tube, forming a short segment of a nanotube with a different helicity. The formation of quantum dots with addimers is particularly favorable for the ( $n,0$ ) zigzag tubes, which are otherwise brittle. This behavior is pro-

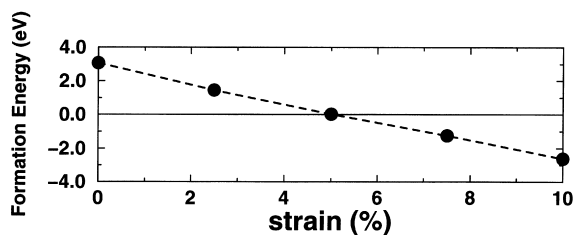


Fig. 2. Formation energy of the (5–7–7–5) defect for the (5,5) tube at different strains.

duced by the changes in the energetics of bond rotations in the vicinity of the addimer. In a zig-zag tube, only the bonds that belong to the newly formed structure can release the strain energy via Stone–Wales rotations. This leads to the appearance of clean armchair inserts in the original zig-zag geometry. The winding of the defect about the nanotube suggests that the combination of addimers plus strain greater than 5% may be a natural way to produce different electronic heterojunctions, thereby leading to the formation of carbon nanotube-based quantum dots.

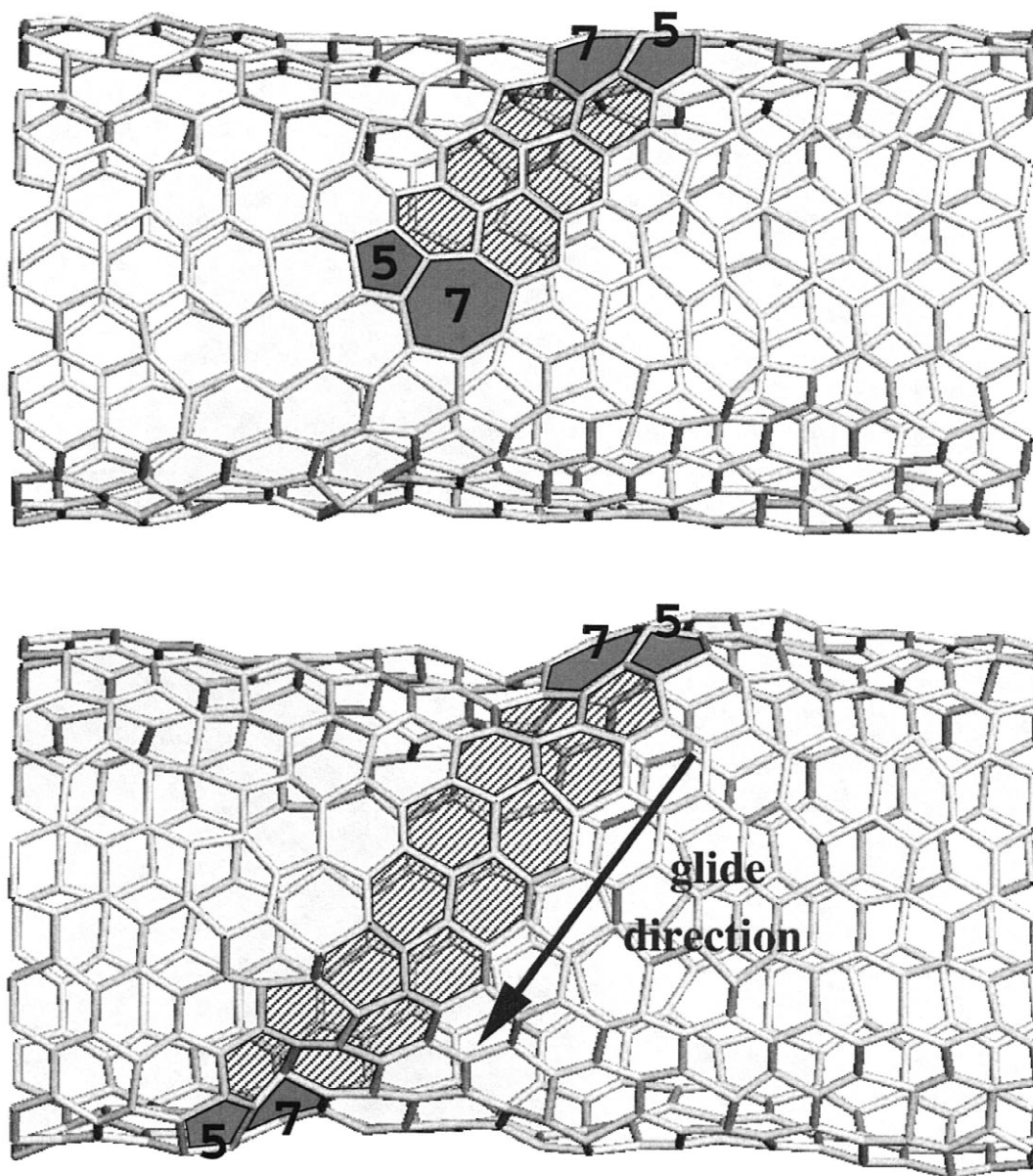


Fig. 3. Plastic deformation of a (10,10) tube under axial tension at 3000 K after 2.5 ns simulation. The shaded area indicates the migration path of the edge dislocations.

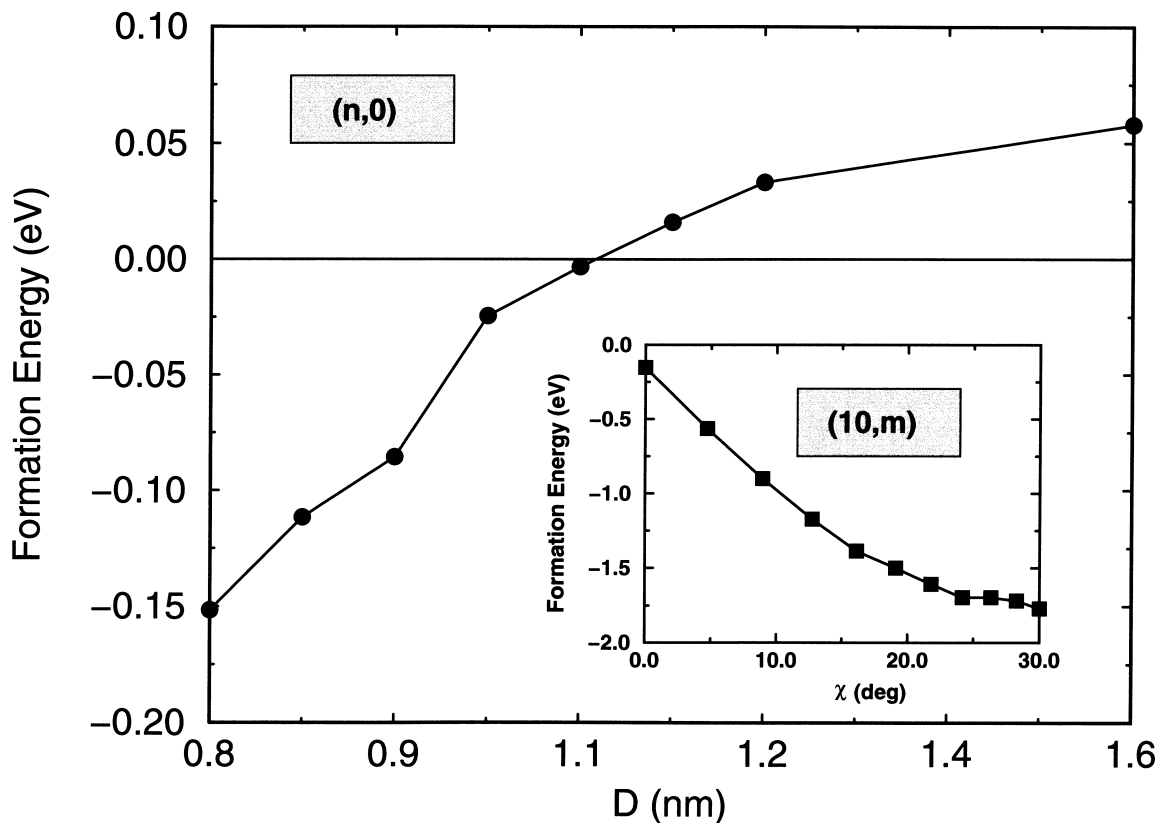


Fig. 4. Formation energy of the off-axis (5–7–7–5) defect in (n,0) tubes of various diameters. In (n,0) tubes,  $D=0.078n$  nm. Inset: formation energy of the off-axis (5–7–7–5) defect in (10,m) tubes of different chiralities. Note that in (n,m) tubes the chiral angle  $\chi = \arctan[\sqrt{3}m/(2n+m)]$  is zero in zig-zag tubes and 30° in armchair tubes. All data refer to 10% strain.

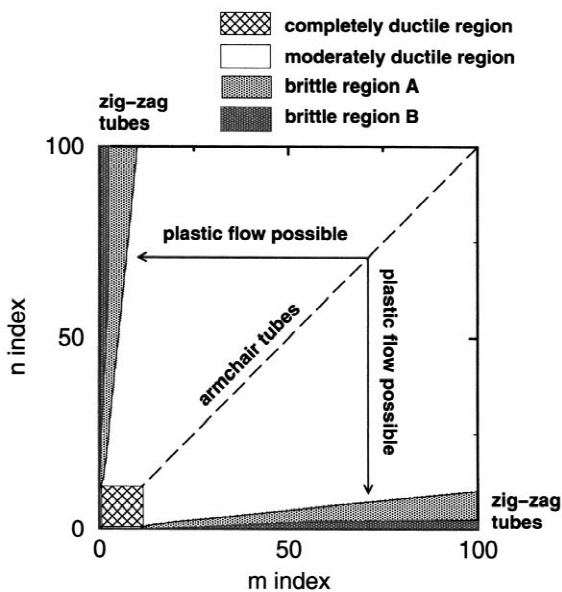


Fig. 5. Ductile–brittle domain map for carbon nanotubes with diameters up to 13 nm. Different shaded areas correspond to different possible behaviors (see text).

### 3. Transport properties

Recently there has been a great amount of research in the field of quantum conductance in carbon nanotubes. Their electronic and transmission properties have been studied both experimentally and theoretically [22–38]. In particular, from the theoretical point of view, the sensitivity of their electronic properties to their geometry makes them truly unique in offering the possibility of studying quantum transport in a very tunable environment. The problem of calculating quantum conductance in carbon nanotubes has been addressed with a variety of techniques that reflect the various approaches in the theory of quantum transport in ballistic systems. Most of the existing calculations derive the electronic structure of a carbon nanotube from a simple  $\pi$ -orbital tight-binding Hamiltonian that describes the bands of the graphitic network via a single nearest-neighbor hopping parameter. Since the electronic properties of carbon nanotubes are basically determined by the  $sp^2$   $\pi$ -orbitals, this model gives a reasonably good qualitative description of their behavior and, given its simplicity, it has become the model of

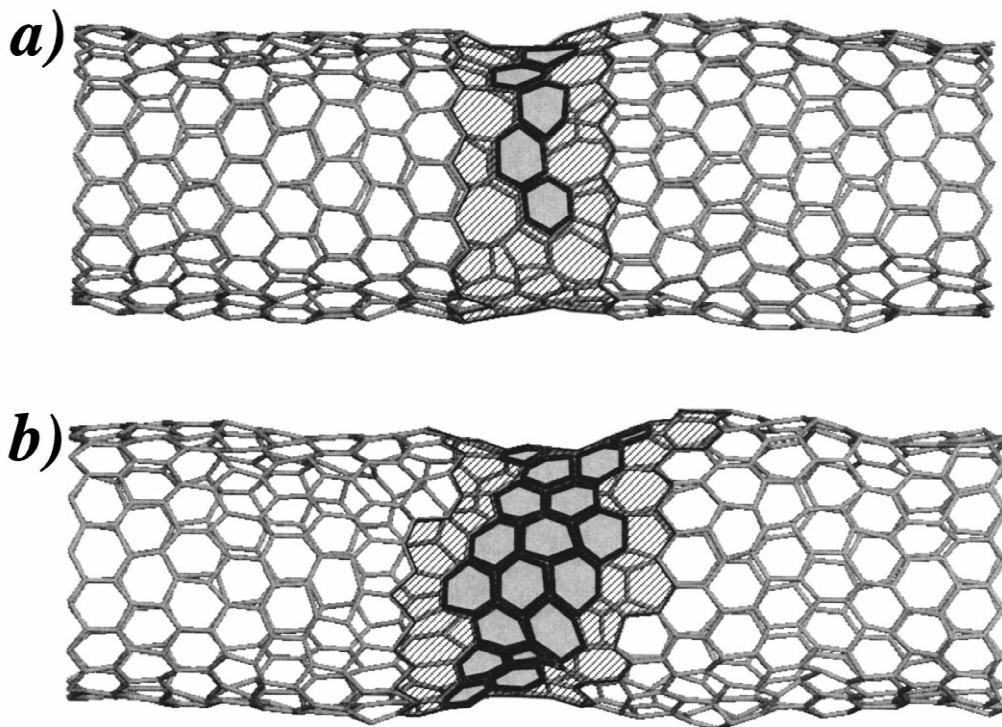


Fig. 6. Time evolution of the (17,0) tube with an addimer under 7.5% strain at 3000 K, illustrating the spontaneous winding of the defect about the tube: (a) the initial configuration consisting of a single turn; (b) the final configuration corresponding to about three turns after 1 ns.

choice in a number of theoretical investigations. However, although qualitatively useful to interpret experimental results, this simple Hamiltonian lacks the accuracy that first principles methods are able to provide.

In the design of all-carbon nanoscale devices, geometrical transformations play a substantial role in modifying the physical properties of the system. These transformations are likely to affect also the electrical properties of the newly designed structures. Recently, we have presented a general scheme for calculating quantum conductance that is particularly suitable for realistic calculations of electronic transport properties in extended systems [39]. This approach is extremely flexible and applicable to any system described by a Hamiltonian with a localized orbital basis. Moreover, the only quantities that enter into the present formulation are the matrix elements of the Hamiltonian operator, with no need for the explicit knowledge of the electron wave functions for the multichannel expansion. The last fact makes the numerical calculations particularly efficient also for systems described by multi-orbital localized-basis Hamiltonians. Our method is based on the Surface Green's Function Matching formalism and efficiently combines the iterative calculation of transfer matrices with the Landauer formula for the coherent conductance. The conductance is related to the current in the tubes via  $I = GV$ , and is given by the Landauer formula

$G = 2e^2/h T$ , where  $T$  is the transmission function [40]. The transmission function is calculated using

$$T = \text{Tr}(\Gamma_L G^r \Gamma_R G^a),$$

where  $G^{r,a}$  represent the retarded and advanced Green's function of the nanotube, and  $\Gamma_{L,R}$  the couplings of the nanotube to the left and right leads, respectively. The Green's function of the conductor as a function of Fermi energy  $\epsilon$  is defined via:

$$G = (\epsilon - H_c - \Sigma_L - \Sigma_R)^{-1},$$

where  $\Sigma_{L,C}$  are the self-energy terms due to the semi-infinite leads, and  $H_c$  the Hamiltonian of the defective nanotube. The self-energy terms also define the couplings  $\Gamma$  through the relation

$$\Gamma_{L,R} = i[\Sigma_{L,R}^r - \Sigma_{L,R}^a].$$

In turn, the self-energy terms are calculated via a surface Green's function matching technique, as previously outlined in the literature [39].

This approach has also been linked with an ab-initio real-space method with a non-orthogonal localized-orbital basis, which has been recently developed in our group. In this way we are now able to compute quantum conduct-

ance in carbon nanotubes in a truly first principle fashion [41,42].

As a first application, we computed the conductance of a (5,5) tube, pristine and with a (5–7–7–5) defect using both ab initio and tight-binding Hamiltonians, as shown in Fig. 7.

The agreement between the two sets of calculation is very good, and gives us confidence of the ability of tight-binding methods to predict quantum conductance of carbon nanotube structures. Moreover, our results for the (5,5) tube with a single (5–7–7–5) defect compare very well with a recent ab initio calculation [37] for a larger (10,10) tube. Using a realistic tight-binding Hamiltonian [43] we have computed quantum conductances of strained tubes. The results show that the defect density plays a key

role in reducing the conductance at the Fermi energy. While the presence of a single defect in a nanotube wall is not likely to produce large changes in the conductance spectrum, as shown before in the case of a (5,5) tube, large defective regions likely to be present in highly strained nanotubes will strongly modify their transport properties. In Fig. 8 we show the conductance spectrum of a deformed nanotube, whose geometry has been obtained in one of our molecular dynamics simulations. The conductance is severely modified by the defective region and in particular a sharp decrease is observed at the Fermi level.

As a last application we investigate the effect that bending has in the transport properties of carbon nanotubes. It has recently been observed [28] that in individual carbon nanotubes deposited on a series of

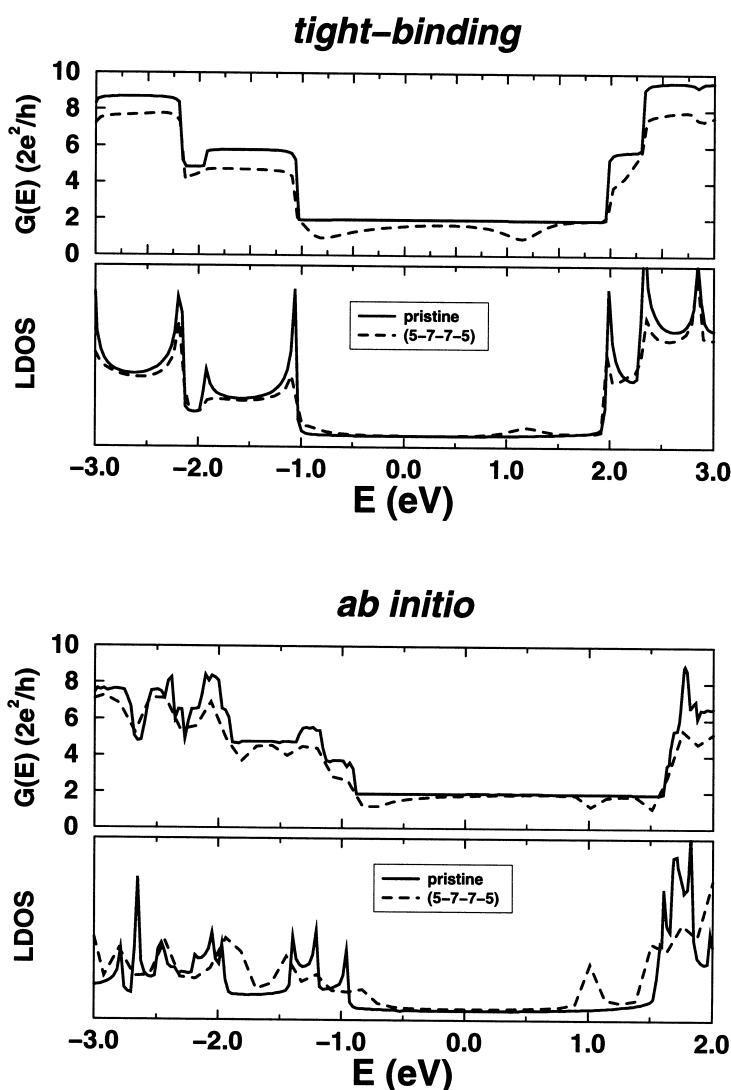


Fig. 7. Lower panel: Ab initio conductance and local density of states for a (5,5) nanotube as pristine and with a (5–7–7–5) defect. Upper panel: Same as above using a tight-binding Hamiltonian.

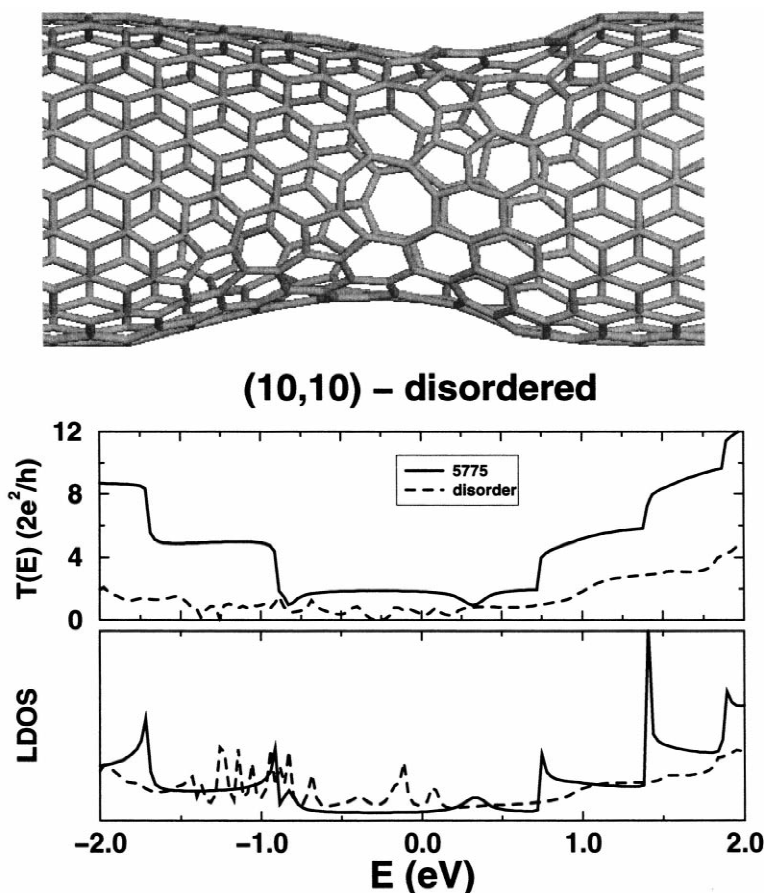


Fig. 8. Upper panel: (10,10) tube at 10% strain after an annealing at 1500 K for 1.0 us. Lower panel: quantum conductance for the above system.

electrodes three classes of behavior can be distinguished: (i) nonconducting at room temperature and below, (ii) conducting at all temperatures, and (iii) partially conducting. The last class represents NTs that are conducting at a high temperature but at a low temperature behave as a chain of quantum wires connected in series. It has been argued that the local barriers in the wire arise from bending of the tube near the edge of the electrodes.

Here we present the results for a small diameter bent (4,4) carbon nanotube. The upper part of Fig. 9 shows the system that we have studied: an initially straight tube has been bent at angles  $\theta$  of  $0^\circ$ ,  $3^\circ$ ,  $6^\circ$  (Fig. 9a,b,c) where  $\theta$  measures the inclination of the two ends of the tubes with respect to the un-bent axis. For  $\theta=6^\circ$  we observe the formation of a kink. Since the formation of kinks in bent carbon nanotubes has been well studied both experimentally and theoretically [1], we do not discuss it here. In the lower part of Fig. 9 we present predictions for the electronic conductance and density of states of the bent tube. The presence of the kink does not alter drastically the local density of states (LDOS) at the interface nor the

conductance of the system. This result suggests that armchair tubes will keep their metallic character irrespective of mechanical deformations and can be identified with the (ii) class of behavior in Ref. [28].

#### 4. Conclusions

In summary, we have shown that in carbon nanotubes high strain conditions can lead to a variety of atomic transformations, often occurring via successive bond rotations. The barrier for the rotation is dramatically lowered by strain, and ab initio results for its strain dependence were presented. While very high strain rates must lead to breakage,  $(n,m)$  nanotubes with  $n, m < 14$  can display plastic flow under suitable conditions. This occurs through the formation of a  $5-7-7-5$  defect, which then splits into two  $5-7$  pairs. The index of the tube changes between the  $5-7$  pairs, potentially leading to metal–semiconductor junctions. A different way to induce transformations is through addimers, which can help form metallic quantum

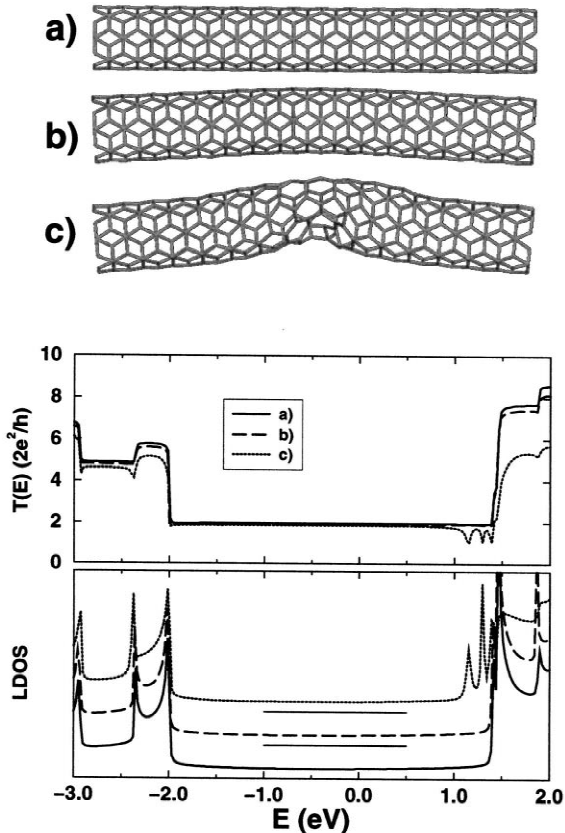


Fig. 9. Upper panel: geometry of the bent (4,4) nanotube used in the calculations. Lower panel: LDOS and quantum conductance for the different geometries:  $\theta = 0^\circ$  (a),  $3^\circ$  (b),  $6^\circ$  (c). LDOSs for different bending angles are shifted in the picture. The Fermi energy is always taken as a reference.

dots in a semiconducting nanotube. We have also computed quantum conductances of strained tubes and defects. The results show that the defect density plays a key role in reducing the conductance at the Fermi energy, and large geometrical deformations highly affect the electrical response of carbon nanotubes. Furthermore, armchair nanotubes can be bent to substantial angles, without significantly affecting the conductance.

## References

[1] Iijima S, Brabec C, Maiti A, Bernholc J. *J Chem Phys* 1996;104:2089.  
 [2] Yakobson BI, Brabec CJ, Bernholc J. *Phys Rev Lett* 1996;76:2511.  
 [3] Despres J, Daguette E, Lafdi K. *Carbon* 1995;33:87.  
 [4] Chopra N, Benedict L, Crespi V, Cohen ML, Louie SG, Zettl A. *Nature* 1995;377:135.  
 [5] Ruoff R, Lorents D. *Bull Am Phys Soc* 1995;40:173.

[6] Briggs EL, Sullivan DJ, Bernholc J. *Phys Rev B* 1995;52:R5471.  
 [7] Briggs EL, Sullivan DJ, Bernholc J. *Phys Rev B* 1996;54:14362.  
 [8] Ceperley D, Alder B. *Phys Rev Lett* 1980;45:566.  
 [9] Bachelet G, Hamann D, Schlüter M. *Phys Rev B* 1982;26:4199.  
 [10] Hamann D, Schlüter M, Chiang C. *Phys Rev Lett* 1979;43:1494.  
 [11] Hamann D. *Phys Rev B* 1989;40:2980.  
 [12] Kleinman L, Bylander D. *Phys Rev Lett* 1982;48:1425.  
 [13] Tersoff J. *Phys Rev Lett* 1988;61:2879.  
 [14] Tersoff J. *Phys Rev B* 1988;37:6991.  
 [15] Brenner DW. *Phys Rev B* 1990;42:9458.  
 [16] Buongiorno Nardelli M, Yakobson BI, Bernholc J. *Phys Rev B* 1998;57:R4277.  
 [17] Buongiorno Nardelli M, Yakobson BI, Bernholc J. *Phys Rev B* 1998;42:4656.  
 [18] Nosé S. *Mol Phys* 1984;52:255.  
 [19] Hoover WG. *Phys Rev A* 1985;31:1695.  
 [20] Martyna GJ, Klein ML, Tuckerman M. *J Chem Phys* 1992;97:2635.  
 [21] Stone AJ, Wales DJ. *Chem Phys Lett* 1986;128:501.  
 [22] Collins PG, Zettl A, Bando H, Thess A, Smalley R. *Science* 1996;278:100.  
 [23] Song SN, Wang XK, Chang RPH, Ketterson JB. *Phys Rev Lett* 1994;72:697.  
 [24] Langer L, Stockman L, Heremans JP et al. *J Mater Res* 1994;9:927.  
 [25] Langer L, Bayot V, Grivei B et al. *Phys Rev Lett* 1996;76:479.  
 [26] Tans SJ, Devoret MH, Dai H et al. *Nature* 1997;386:474.  
 [27] Bachtold A, Strunk C, Salvetat J-P et al. *Nature* 1999;397:673.  
 [28] Bezryadin A, Verschueren ARM, Tans SJ, Dekker C. *Phys Rev Lett* 1998;80:4036.  
 [29] Paulson S, Falvo MR, Snider N et al. <http://xxx.lanl.gov/abs/cond-mat/9905304>, preprint, 1999.  
 [30] Tian W, Datta S. *Phys Rev B* 1994;49:5097.  
 [31] Saito R, Dresselhaus G, Dresselhaus MS. *Phys Rev B* 1996;53:2044.  
 [32] Chico L, Benedict LX, Louie SG, Cohen ML. *Phys Rev B* 1996;54:2600.  
 [33] Tamura R, Tsukada M. *Phys Rev B* 1997;55:4991.  
 [34] Tamura R, Tsukada M. *Phys Rev B* 1998;58:8120.  
 [35] Anantran MP, Govindan TR. *Phys Rev B* 1998;58:4882.  
 [36] Farajian AA, Esfarjani K, Kawazoe Y. *Phys Rev Lett* 1999;82:5084.  
 [37] Choi HJ, Ihm J. *Phys Rev B* 1999;59:2267.  
 [38] Rochefort A, Lesage F, Salahub DR, Avouris P. <http://xxx.lanl.gov/abs/condmat/9904083>, preprint, 1999.  
 [39] Buongiorno Nardelli M. *Phys Rev B* 1999;60:7828.  
 [40] Datta S. *Electronic transport in mesoscopic systems*, Cambridge: University Press, 1995.  
 [41] Fattebert J-L, Bernholc J. To be published.  
 [42] Buongiorno Nardelli M, Fattebert J-L, Bernholc J. To be published.  
 [43] Charlier JC, Lambin Ph, Ebbesen TW. *Phys Rev B* 1996;54:R8377.